This article has been accepted for inclusion in a future issue of this journal. Content is final as presented, with the exception of pagination.

A Mathematical Model for the Analysis of Jet Engine Fuel Consumption During Aircraft Climb and Descent

Francisco Velásquez-SanMartín, Xabier Insausti, Marta Zárraga-Rodríguez, and Jesús Gutiérrez-Gutiérrez, *Senior Member, IEEE*

***Abstract*— This paper proposes a mathematical model that studies the fuel consumption of a jet engine aircraft during the climbing and descent flight phases. Such problem is addressed by providing a closed-form formula of the aircraft's rate-of-climb and rate-of-descent, which then enables obtaining a closed-form formula of the aircraft's fuel consumption that provides the closed-form relationship between the aircraft's fuel consumption and aerodynamic, engine and design parameters. In order to validate our mathematical model, a comparison is made between our results and results provided by Piano-X software and accuracy between both is proven. Furthermore, our mathematical model is applied to the calculation of pollutant gas emissions, specifically, we present a closed-form expression that provides the dependency between the mass of pollutant gas emitted and the aircraft's aerodynamic, engine and design parameters.**

***Index Terms*— Aircraft rate-of-climb, aircraft rate-of-descent, aircraft fuel consumption, pollutant gas emissions.**

I. Introduction

THROUGHOUT its history, the aviation industry sector has evolved enduring a series of important challenges brought by the globalization phenomena. Airlines need to cover the demand of national or international routes with its aircraft fleet capacity. Fulfilling passenger satisfaction and minimizing flight operational costs is a fundamental challenge.

As for air traffic management (ATM), another challenge is to optimize taxi-out and taxi-in times of departing and arriving flights in high activity airports or to control air traffic under uncertain weather conditions. Likewise, several regulatory agencies (such as the IATA, ICAO, FAA, among others) seek not only to ensure airspace safety, but also tackle climate change. Climate change is a problem that concerns the whole aviation industry sector and it has been, and still remains, one of the most critical challenges to be addressed.

Pollutant gas emissions due to aircraft fuel consumption accounts for a considerable share in the contribution to climate change. According to [1], between 2005 and 2019, the worldwide fuel consumption of commercial airlines increased from 68 to 95 billions of gallons, and expects to continue rising due to the worldwide surge of passengers [2]. In 2019, a total of 915 million tons of carbon dioxide (CO_2) were emitted to the atmosphere by the aviation industry sector, which corresponds to a 12% of the CO_2 emissions produced by the general transportation sector [3].

In order to cope with such problem, numerous measures have been taken by airlines such as giving periodic maintenance to its aircraft fleet engines, adopting the use of sustainable aviation fuels (SAFs) and upgrading its aging aircraft fleet with modern efficient aircraft.

Aircraft and engine manufacturers provide special aid in this issue with technological advancements such as aircraft fuselage and wing geometries that offer better aerodynamic performance or the turbofan engine, which has considerably reduced aircraft fuel consumption. Moreover, the ATM provides airlines with the optimal and safest flight routes which helps reducing the flights operational costs, and the pollutant gas emissions.

This measures have brought a significant impact in reducing aircraft fuel consumption and consequently, the mass of pollutant gases emitted to the atmosphere. However, being able to quantify how much fuel is consumed by an specific aircraft covering a particular route would enable knowing the associated fuel costs to such aircraft and route.

Aircraft performance plays a key role in calculating the fuel consumption of a jet engine aircraft since it's a discipline that studies the behavior of an aircraft flying. Such behavior is characterized by the interaction of the aircraft's state variables subject to the equations of motion of the different flight phases (take-off, climb, cruise, descent and landing). Among the aircraft's state variables, it is known that the fuel flow rate provides the mass of fuel consumed per unit of time, which ultimately leads to knowing the total amount of fuel consumed during each flight phase, and therefore, its associated fuel costs.

Existing computer programs and manuals such as ACSYNT, FLOPS, DATCOM, BADA, ESDU and PIANO (see [4, p. 9]) are commonly employed in aircraft preliminary design, stability and control, and performance analyses. Focusing on the aircraft performance analysis, such computer programs and manuals rely on numerical methods or on energy balance methods in order to solve the equations of motion for the different flight phases.

Manuscript received 27 July 2022; revised 13 March 2023 and 30 August 2023; accepted 30 October 2023. This work was supported in part by the Basque Government through the CODISAVA2 Project under Grant KK-2020/00044. The Associate Editor for this article was B. F. Ciuffo. *(Corresponding author: Francisco Velásquez-SanMartín.)*

The authors are with the Department of Biomedical Engineering and Sciences, Tecnun, University of Navarra, 20018 Donostia-San Sebastián, Spain (e-mail: fjvelasquez@tecnun.es).

Digital Object Identifier 10.1109/TITS.2023.3333276

1558-0016 © 2023 IEEE. Personal use is permitted, but republication/redistribution requires IEEE permission.
See https://www.ieee.org/publications/rights/index.html for more information.

Authorized licensed use limited to: TECNUN-UNIVERSIDAD DE NAVARRA. Downloaded on February 12,2024 at 08:33:46 UTC from IEEE Xplore. Restrictions apply.

This article has been accepted for inclusion in a future issue of this journal. Content is final as presented, with the exception of pagination.

Several studies have approached the problem of calculating aircraft fuel consumption. In [5] aircraft fuel consumption is calculated based on the energy balance method. In [6], [7], [8], [9], and [10] aircraft fuel consumption is calculated based on statistical learning algorithms. Other studies (see, e.g., [11], [12], [13], [14]), apply statistical techniques to data obtained from the aircraft's flight data recorder (FDR) in order to address the problem of estimating aircraft fuel consumption. Examples of the energy assessment and environmental impact of jet engine fuel consumption can be found in [15] and [16]. In addition, further studies that address the modeling of aircraft flight phases can be found in [17], [18], and [19].

The accuracy of such numerical, energy balance and statistical methods has thoroughly improved by performing complex and large-scale simulations at a low computational cost. Nevertheless, such methods do not provide a closed-form solution of the equations of motion of an aircraft during its different flight phases. The novelty of this paper is to find a closed-form solution that provides:

- the relationship between the aircraft's state variables and aerodynamic, engine and design parameters and,
- the possibility of performing sensibility and optimization analyses in order to better understand the behavior of the physical system under consideration.

In [20] and [21], a mathematical model for the take-off and cruising flight phases can be found, respectively. In this paper, we propose a mathematical model for the climbing and descent flight phases. The model leads to a first order non-linear ordinary differential equation of the aircraft's rate-of-climb and rate-of-descent variation over time, respectively.

Our aim is to find a closed-form solution of such differential equations, which ultimately lead to a closed-form formula of the aircraft's fuel consumption. Specifically, such closed-form solutions provide a closed-form relationship, over time, of the aircraft's rate-of-climb, rate-of-descent and fuel consumption with aerodynamic engine and design parameters.

Our mathematical model is validated with an example case of a Boeing 767-300ER under given climb and descent conditions provided by the *Piano-X Aircraft Emissions and Performance* software [22]. Relevant studies that have made use of the Piano-X software can be found in [23], [24], [25], [26], [27], and [28].

The rest of the paper is organized as follows: Section II presents the problem, Section III presents the closed-form formula of the aircraft's rate-of-climb, rate-of-descent and fuel consumption. Section IV compares the values of the aircraft's rate-of-climb, rate-of-descent, fuel consumption provided by our mathematical model and the ones provided by the Piano-X software. Section V is devoted to the application of the mathematical model for the calculation of pollutant gas emissions. Finally, Section VI concludes the paper.

II. Problem Statement

The physical system analyzed consists of a modern jet engine aircraft during the climbing and descent phases. Due to the aircraft's altitude variation over time and fuel consumption, the behavior of the aircraft during such flight phases cannot be considered steady. For each flight phase, our aim is to find a first order non-linear differential equation and to obtain a closed-form solution of such differential equation, which ultimately leads to a closed-form formula for the aircraft's fuel consumption.

The International Standard Atmospheric (ISA) model, along with the equations of motion, equations for the aircraft's thrust specific fuel consumption (TSFC) and thrust, provide the basis of the mathematical model. The following assumptions are made in order to develop the mathematical model:

- The aircraft is a variable-mass system due to engine fuel consumption.
- The ISA model is a static atmosphere model which enables considering thermodynamic parameters such as air temperature, pressure and density as a function of altitude.
- Regarding aircraft flight mechanics:
  - The climbing flight phase takes place between the take-off and cruising flight phases and consists of gradual climb segments in which a desired altitude is attained at a constant angle of climb.
  - The descent flight phase takes place between the cruising and landing flight phases and consists of gradual descent segments in which a desired altitude is attained at a constant angle of descent.
  - For the climbing and descent flight phases, the aircraft's velocity vector remains constant in direction (due to the constant angle of climb and descent, respectively) but not in magnitude.
  - A vertical mass symmetry plane along the aircraft's longitudinal axis contains all the interacting forces and the velocity vector.
  - The aircraft's thrust specific fuel consumption and thrust are referred to the uninstalled values.
  - The values of the lift and drag coefficients are based on the aircraft's wing area.
  - Wind effects are not taken into account.
- Regarding aircraft pollutant gas emissions:
  - Carbon dioxide emissions are specifically addressed due to the complex nature of modulating emission characteristics of other pollutant compounds and their geographically varying atmospheric conditions.

In Section IV we show that, although considering the above assumptions, the fuel consumption provided by our mathematical model is very close to the fuel consumption given by the Piano-X software, whose results are proven to be close to reality. Therefore, we conclude that our mathematical model provides results close to reality.

A. Atmospheric Model

We are interested in defining the air density and speed of sound as functions of altitude since the aircraft's state variables, during the climbing and descent flight phases, can be expressed as altitude-dependent functions.

A summary of the ISA model equations, including the air temperature and pressure, can be found in [29, pp. 81-83].

Authorized licensed use limited to: TECNUN-UNIVERSIDAD DE NAVARRA. Downloaded on February 12,2024 at 08:33:46 UTC from IEEE Xplore. Restrictions apply.

This article has been accepted for inclusion in a future issue of this journal. Content is final as presented, with the exception of pagination.

The air density $\rho(h)$ is defined as

$$\rho(h) = \rho_0 \left(1 - \frac{L}{T_0} h\right)^{\beta}, \tag{1}$$

where $\rho_0 = 1.2250$ kg/m^3 is the density at sea-level, $T_0 = 288.15$ K the sea-level temperature and $L = 0.0065$ K/m the temperature gradient up to the troposphere (that is, for $h < 11,000$ m). For simplicity, we denote the term L/T_0 as α.

The parameter $\beta = g\mathcal{M}/RL - 1$ is considered constant, where $g = 9.80665$ m/s^2 represents the gravitational acceleration, $\mathcal{M} = 0.0289652$ kg/mol is the molar mass, and $R = 8.31446$ J/(mol K) is the ideal gas constant.

The speed of sound $a(h)$ is defined as

$$a(h) = a_0 \left(1 - \alpha h\right)^{1/2}, \tag{2}$$

where $a_0 = 340.3$ m/s is the sea-level speed of sound.

B. Equations for the Mathematical Model - Climbing Flight Phase

Let us denote the aircraft's altitude $h(t) > 0$ as h and the aircraft's rate-of-climb $dh/dt > 0$ as η.

We define the aircraft's weight $W(h, \eta)$ as proposed in [30, p. 406]:

$$W(h, \eta) = W_0 + W_f(h, \eta), \tag{3}$$

being W_0 the constant weight term, which includes the operating empty and payload weights, and $W_f(h, \eta)$ the time-varying term that represents the fuel weight, that is, $W_f(t) = m_f(h, \eta)g$, where $m_f(h, \eta)$ is the fuel mass.

The definition of the fuel consumption relationship is given as

$$\frac{dm_f}{dt} = -c_j(h, \eta) F_N(h, \eta), \tag{4}$$

where dm_f/dt represents the fuel flow rate, which is the mass of fuel consumed per unit of time, $c_j(h, \eta)$ is the thrust specific fuel consumption and $F_N(h, \eta)$ the aircraft's thrust.

According to [31, pp. 66, 75],

$$c_j(h, \eta) = c(1 - 0.15\lambda^{0.15}) \left(1 + 0.28(1 + 0.063\lambda^2) M(h, \eta)\right) \times \left(\frac{\rho(h)}{\rho_0}\right)^m \tag{5}$$

and

$$F_N(h, \eta) = N_e F_{N,0} \left((f_1 + f_2\lambda) + (f_3 + f_4\lambda) M(h, \eta)\right) \times \left(\frac{\rho(h)}{\rho_0}\right)^n, \tag{6}$$

where $c = 2 \cdot 10^{-5}$ (kg/s)/N, $\lambda > 0$ is the jet engine by-pass ratio (BPR), $M(h, \eta)$ is the Mach number, $N_e > 0$ is the number of engines, $F_{N,0} > 0$ the aircraft's static thrust for the climbing flight phase, f_i (with $i = \{1, 2, 3, 4\}$) are specific parameters that can be found in [31, p. 67] and $m = 0.08$, $n = 0.7$ (see [31, pp. 67, 75]). The Mach number $M(h, \eta)$ is given by

$$M(h, \eta) = \frac{v(\eta)}{a(h)}, \tag{7}$$

where $v(\eta)$ represents the aircraft's velocity which is defined as

$$v(\eta) = \frac{\eta}{\sin(\gamma)}, \tag{8}$$

with γ $(0 < \gamma < \pi/2)$ being the aircraft's climbing angle. From Eqs. (7) and (8) we have

$$M(h, \eta) = \frac{\eta}{a(h)\sin(\gamma)}. \tag{9}$$

Using Eq. (9), Eqs. (5) and (6) can be written as

$$c_j(h, \eta) = \left(\zeta_1 + \zeta_2 \frac{\eta}{a(h)}\right) (\rho(h))^m \tag{10}$$

and

$$F_N(h, \eta) = \left(F_1 + F_2 \frac{\eta}{a(h)}\right) (\rho(h))^n, \tag{11}$$

where

$$\zeta_1 = c(1 - 0.15\lambda^{0.15})\rho_0^{-m},$$
$$\zeta_2 = \frac{0.28\zeta_1}{\sin(\gamma)}(1 + 0.063\lambda^2),$$

and

$$F_1 = N_e F_{N,0}(f_1 + f_2\lambda)\rho_0^{-n},$$
$$F_2 = \frac{N_e F_{N,0}}{\sin(\gamma)}(f_3 + f_4\lambda)\rho_0^{-n}. \tag{12}$$

From [32, p. 311], the equations of motion for the climbing phase are

$$F_N(h, \eta) - D(h, \eta) - W(h, \eta)\sin(\gamma) = \frac{W(h, \eta)}{g}\frac{dv}{dt}, \tag{13}$$

and

$$L(h, \eta) = W(h, \eta)\cos(\gamma), \tag{14}$$

where the aerodynamic forces, lift $L(h, \eta)$ and drag $D(h, \eta)$, are defined as

$$L(h, \eta) = \rho(h)\left(v(\eta)\right)^2 \frac{Ac_L}{2} \tag{15}$$

and

$$D(h, \eta) = \rho(h)\left(v(\eta)\right)^2 \frac{Ac_D}{2}, \tag{16}$$

with A being aircraft's wing area, $c_L > 0$ the lift coefficient and $c_D > 0$ the drag coefficient. Considering the definition of the aircraft's velocity provided by Eq. (8), the lift and drag forces can be expressed as

$$L(h, \eta) = \rho(h)\eta^2 \frac{Ac_L}{2\sin^2(\gamma)} \tag{17}$$

and

$$D(h, \eta) = \rho(h)\eta^2 \frac{Ac_D}{2\sin^2(\gamma)}. \tag{18}$$

We now obtain the first order non-linear ordinary differential equation for the climbing flight phase.

By combining (13) and (14) we have

$$F_N(h, \eta) = L(h, \eta)\left(\frac{1}{g\cos(\gamma)}\frac{dv}{dt} + \tan(\gamma) + \frac{1}{E}\right), \tag{19}$$

where $E = L(h, \eta)/D(h, \eta) = c_L/c_D$.

Authorized licensed use limited to: TECNUN-UNIVERSIDAD DE NAVARRA. Downloaded on February 12,2024 at 08:33:46 UTC from IEEE Xplore. Restrictions apply.

This article has been accepted for inclusion in a future issue of this journal. Content is final as presented, with the exception of pagination.

From (8) we have

$$\frac{dv}{dt} = \frac{1}{\sin(\gamma)}\frac{d\eta}{dt}. \tag{20}$$

By combining (17), (19) and (20) we obtain

$$F_N(h,\eta) = \frac{\rho(h)\eta^2}{\mathcal{S}}\left(\frac{1}{\omega}\frac{d\eta}{dt} + \tan(\gamma) + \frac{1}{E}\right), \tag{21}$$

where $\mathcal{S} = 2\sin^2(\gamma)/Ac_L$ and $\omega = g\sin(\gamma)\cos(\gamma)$. Combining (11) and (21) brings

$$\mathcal{S}\left(\rho(h)\right)^{n-1}\eta^{-2}\left(F_1 + F_2\frac{\eta}{a(h)}\right) = \frac{1}{\omega}\frac{d\eta}{dt} + \tan(\gamma) + \frac{1}{E},$$

which can be expressed as

$$\omega\mathcal{S}F_1\left(\rho(h)\right)^{n-1} + \omega\mathcal{S}F_2\left(\frac{(\rho(h))^{n-1}}{a(h)}\right)\eta - \omega\left(\tan(\gamma) + \frac{1}{E}\right)\eta^2 = \eta^2\frac{d\eta}{dt}. \tag{22}$$

By substituting (1) and (2) in (22) we obtain

$$\kappa_1(1-\alpha h)^q + \kappa_2(1-\alpha h)^r\eta + \kappa_3\eta^2 = \eta^2\frac{d\eta}{dt}, \tag{23}$$

where $q = (n-1)\beta$ and $r = q - 1/2$ are non-integer numbers and

$$\kappa_1 = \omega\mathcal{S}F_1\rho_0^{n-1}, \quad \kappa_2 = \omega\mathcal{S}F_2\frac{\rho_0^{n-1}}{a_0}, \quad \kappa_3 = -\omega\left(\tan(\gamma) + \frac{1}{E}\right). \tag{24}$$

For the climbing flight phase, Eq. (23) represents our sought first order non-linear ordinary differential equation whose closed-form solution is not known. In Section III, we will solve Eq. (23) piecewise to obtain for each piece a closed-form solution which will also provide the closed-form formula of the aircraft's fuel consumption during the climbing phase.

C. Equations for the Mathematical Model - Descent Flight Phase

In this flight phase, the aircraft's rate-of-descent $\eta < 0$. Also, let the definitions provided in Eqs. (3)–(12) and Eq. (14) remain valid for the descent flight phase, with γ $(-\pi/2 < \gamma < 0)$ being the aircraft's descent angle.

Regarding the equations of motion, it is known from [29, p. 334] that

$$F_N(h,\eta) - \psi D(h,\eta) - W(h,\eta)\sin(\gamma) = \frac{W(h,\eta)}{g}\frac{dv}{dt}, \tag{25}$$

where ψ $(0 < \psi < 1)$ accounts for the spillage drag effect [33, pp. 503-505].

We now obtain the first order non-linear ordinary differential equation for the descent flight phase.

By combining (14), (17), (20) and (25) we have

$$F_N(h,\eta) = \frac{\rho(h)\eta^2}{\mathcal{S}}\left(\frac{1}{\omega}\frac{dv}{dt} + \tan(\gamma) + \frac{\psi}{E}\right). \tag{26}$$

Substituting (11) in (26) and reordering terms brings

$$\omega\mathcal{S}F_1\left(\rho(h)\right)^{n-1} + \omega\mathcal{S}F_2\left(\frac{(\rho(h))^{n-1}}{a(h)}\right)\eta - \omega\left(\tan(\gamma) + \frac{\psi}{E}\right)\eta^2 = \eta^2\frac{d\eta}{dt}. \tag{27}$$

Notice that (27) has a similar form as (22). By substituting (1) and (2) in (27) we obtain

$$\kappa_1(1-\alpha h)^q + \kappa_2(1-\alpha h)^r\eta + \kappa_3\eta^2 = \eta^2\frac{d\eta}{dt}, \tag{28}$$

which is the same expression as (23), with the values of κ_1 and κ_2 given in (24) and with

$$\kappa_3 = -\omega\left(\tan(\gamma) + \frac{\psi}{E}\right). \tag{29}$$

As for the climbing flight phase, the closed-form solution of Eq. (28) is not known. In Section III, we will solve Eq. (28) piecewise to obtain for each piece a closed-form solution which will also provide the closed-form formula of the aircraft's fuel consumption during the descent phase.

III. Closed-Form Solution of the Aircraft's Fuel Consumption

In this section, we divide the climbing and descent flight phases in altitude segments in which the air density and speed of sound are considered constant, that is, $\rho(h) = \rho$ and $a(h) = a$, this allows us to obtain a closed-form solution for Eqs. (23) and (28) piecewise.

For each piece, the sought first order ordinary differential equation can be written as

$$\mathsf{k}_1 + \mathsf{k}_2\eta + \mathsf{k}_3\eta^2 = \eta^2\frac{d\eta}{dt}, \tag{30}$$

where

$$\mathsf{k}_1 = \omega\mathcal{S}F_1\rho^{n-1}, \quad \mathsf{k}_2 = \omega\mathcal{S}F_2\frac{\rho^{n-1}}{a}, \tag{31}$$

and for the climbing flight phase

$$\mathsf{k}_3 = -\omega\left(\tan(\gamma) + \frac{1}{E}\right), \tag{32}$$

whereas for the descent flight phase

$$\mathsf{k}_3 = -\omega\left(\tan(\gamma) + \frac{\psi}{E}\right). \tag{33}$$

Since

$$\frac{dm_f}{dt} = \frac{dm_f}{d\eta}\frac{d\eta}{dt}, \tag{34}$$

from (4), (10), (11) and (30) yields

$$\frac{dm_f}{d\eta} = -\rho^{m+n}\frac{(\zeta_1 + (\zeta_2/a)\eta)(F_1 + (F_2/a)\eta)\eta^2}{\mathsf{k}_1 + \mathsf{k}_2\eta + \mathsf{k}_3\eta^2}, \tag{35}$$

whenever $\mathsf{k}_1 + \mathsf{k}_2\eta + \mathsf{k}_3\eta^2 \neq 0$.

By using (30) and (35), we now obtain a closed-form solution of the aircraft's fuel consumption for each altitude segment.

Authorized licensed use limited to: TECNUN-UNIVERSIDAD DE NAVARRA. Downloaded on February 12,2024 at 08:33:46 UTC from IEEE Xplore. Restrictions apply.

This article has been accepted for inclusion in a future issue of this journal. Content is final as presented, with the exception of pagination.

We assume that an altitude segment starts at time instant t_s and ends at time instant t_e, and the rate-of-climb or rate-of-descent η is obtained from (30) as follows:

$$\begin{aligned} t_e - t_s &= \int_{t_s}^{t_e} dt = \int_{t_s}^{t_e} \frac{\eta^2}{\mathsf{k}_1 + \mathsf{k}_2\eta + \mathsf{k}_3\eta^2}\left(\frac{d\eta}{dt}\right) dt \\ &= \int_{\eta_s}^{\eta_e} \frac{\eta^2}{\mathsf{k}_1 + \mathsf{k}_2\eta + \mathsf{k}_3\eta^2} d\eta \\ &= \frac{1}{\mathsf{k}_3}\left((\eta_e - \eta_s) + \frac{r_1^2}{r_1 - r_2}\ln\left|\frac{\eta_e - r_1}{\eta_s - r_1}\right|\right) \\ &\quad - \frac{1}{\mathsf{k}_3}\left(\frac{r_2^2}{r_1 - r_2}\ln\left|\frac{\eta_e - r_2}{\eta_s - r_2}\right|\right), \end{aligned} \tag{36}$$

where $\eta_s = \eta(t_s)$ and $\eta_e = \eta(t_e)$ are the starting and the ending rate-of-climb or rate-of-descent, respectively, and

$$\begin{aligned} r_1 &= \frac{-\mathsf{k}_2 - \sqrt{\mathsf{k}_2^2 - 4\mathsf{k}_1\mathsf{k}_3}}{2\mathsf{k}_3}, \\ r_2 &= \frac{-\mathsf{k}_2 + \sqrt{\mathsf{k}_2^2 - 4\mathsf{k}_1\mathsf{k}_3}}{2\mathsf{k}_3}, \end{aligned} \tag{37}$$

whenever $r_1, r_2 \notin [\eta_s, \eta_e]$.[1]

The amount of consumed fuel mass is obtained from (35) as follows:

$$\begin{aligned} m_f(\eta_e) - m_f(\eta_s) &= \int_{\eta_s}^{\eta_e}\left(\frac{dm_f}{d\eta}\right) d\eta \\ &= \int_{\eta_s}^{\eta_e} -\rho^{m+n}\frac{(\zeta_1 + (\zeta_2/a)\eta)\,(F_1 + (F_2/a)\eta)\,\eta^2}{\mathsf{k}_1 + \mathsf{k}_2\eta + \mathsf{k}_3\eta^2} d\eta \\ &= -\frac{\rho^{m+n}}{\mathsf{k}_3}\left(\epsilon_1(\eta_e - \eta_s) + \epsilon_2(\eta_e^2 - \eta_s^2) + \epsilon_3(\eta_e^3 - \eta_s^3)\right) \\ &\quad - \frac{\rho^{m+n}}{\mathsf{k}_3}\left(\epsilon_4\ln\left|\frac{\eta_e - r_1}{\eta_s - r_1}\right| - \epsilon_5\ln\left|\frac{\eta_e - r_2}{\eta_s - r_2}\right|\right), \end{aligned} \tag{38}$$

where

$$\begin{aligned} \epsilon_1 &= \frac{F_2\zeta_2}{a^2}(r_1^2 + r_1r_2 + r_2^2) + \frac{1}{a}(\zeta_1F_2 + \zeta_2F_1)(r_1 + r_2) + F_1\zeta_1, \\ \epsilon_2 &= \frac{F_2\zeta_2}{2a^2}(r_1 + r_2) + \frac{1}{2a}(\zeta_1F_2 + F_1\zeta_2), \\ \epsilon_3 &= \frac{F_2\zeta_2}{3a^2}, \\ \epsilon_4 &= \frac{r_1^2}{r_1 - r_2}\left(F_1 + \frac{F_2}{a}r_1\right)\left(\zeta_1 + \frac{\zeta_2}{a}r_1\right), \\ \epsilon_5 &= \frac{r_2^2}{r_1 - r_2}\left(F_1 + \frac{F_2}{a}r_2\right)\left(\zeta_1 + \frac{\zeta_2}{a}r_2\right), \end{aligned}$$

whenever $r_1, r_2 \notin [\eta_s, \eta_e]$.

In Section IV an example case of a Boeing 767-300ER during the climbing and descent flight phases is presented. The numerical solutions of (23) and (28) are shown along with the closed-form solution (36), and the fuel consumption for each of the climbing and descent segments is obtained through (38). Agreement between the results of our mathematical model and the results provided by the Piano-X software confirm the accuracy of our mathematical model.

[1] In Appendix A we show that, for the climbing flight phase, $r_1 > 0$ and $r_2 < 0$.

TABLE I

A SUMMARY OF THE INPUT PARAMETERS FOR THE SIMULATION. THE FUEL MASS AT THE BEGINNING OF THE CLIMBING AND DESCENT SEGMENTS IS REPRESENTED BY $m_f(h_0, \eta_0)$

Flight Phase	h_0 (m)	h_f (m)	η_0 (m/s)	W_0 (N)	$m_f(h_0, \eta_0)$ (kg)
Climbing	3,048	5,448	19.83	1,327,046	23,988
Descent	8,848	7,016	−13.40	1,096,825	5,261

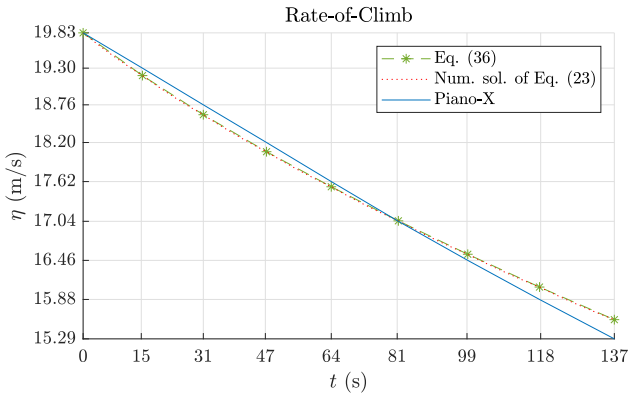

Fig. 1. The aircraft's rate-of-climb is represented for our mathematical model and Piano-X.

IV. EXAMPLE CASE: VALIDATION AND DISCUSSION

In this section we present an example case of a jet engine aircraft during the climbing and descent flight phases in order to validate our mathematical model. A comparison is made between our mathematical model and the Piano-X software for the aircraft's rate-of-climb, rate-of-descent, and fuel consumption. The selected aircraft is the Boeing 767-300ER, which is freely available in the Piano-X aircraft database.

An example route of 2,145 nautical miles (nmi) was simulated in Piano-X. From the climbing flight phase of such simulation, we focus on the climbing segment that goes from $h_0 = 3,048$ m to $h_f = 5,448$ m of altitude. As for the descent flight phase, we focus on the descent segment that goes from $h_0 = 8,848$ m to $h_f = 7,016$ m of altitude. A summary of the input parameters for the simulation are given in Table I, and further details about the Piano-X configuration can be found in Appendix B. Data from the Boeing 767-300ER was obtained from [34] and [35], where the jet engine features correspond to the CF6-80C2B2 model [36], which are $\lambda = 5.31$ and $F_{N,0} = 162.5$ kN.

As stated in Section III, (36) is the piecewise closed-form solution of (23) and (28). Tables II and III present the values of such piecewise closed-form solutions and the corresponding values provided by Piano-X, for the climbing and descent flight phases, respectively.

In Figure 1, the piecewise closed-form solution given by (36) is compared with the numerical solution of (23) and with the values of the aircraft's rate-of-climb provided by Piano-X. The numerical solution of (23) was computed employing the `ode45` numerical solver of MATLAB®. It is interesting to observe the close proximity between the piecewise solution (36) and the numerical solution of (23). In fact, the maximum relative difference between both occurs at $t_f = 137$ s and

Authorized licensed use limited to: TECNUN-UNIVERSIDAD DE NAVARRA. Downloaded on February 12,2024 at 08:33:46 UTC from IEEE Xplore. Restrictions apply.

This article has been accepted for inclusion in a future issue of this journal. Content is final as presented, with the exception of pagination.

TABLE II

VALUES OF THE CONSIDERED PIECEWISE SOLUTION DURING CLIMB. THE VALUES OF γ AND E ARE THE CLIMBING ANGLE AND LIFT-TO-DRAG RATIO AT THE BEGINNING OF EACH PIECE, RESPECTIVELY, AND ρ AND a ARE THE MEAN VALUES OF THE AIR DENSITY AND SPEED OF SOUND OF EACH PIECE

Piece	γ (rad)	E (-)	ρ (kg/m^3)	a (m/s)	t_s (s)	t_e (s)	η_s (m/s)	η_e (m/s)	$\eta_{\text{Piano-X}}$ (m/s)	
1	0.1115	17.67	0.8908	327.8	0.0	15.3	19.83	19.20	19.83	19.30
2	0.1070	17.69	0.8635	326.6	15.3	31.0	19.20	18.62	19.30	18.76
3	0.1025	17.71	0.8368	325.4	31.0	47.3	18.62	18.08	18.76	18.20
4	0.0980	17.73	0.8108	324.2	47.3	64.0	18.08	17.56	18.20	17.62
5	0.0935	17.75	0.7854	323.0	64.0	81.3	17.56	17.05	17.62	17.04
6	0.0891	17.77	0.7606	321.8	81.3	99.2	17.05	16.56	17.04	16.46
7	0.0848	17.79	0.7364	320.5	99.2	117.7	16.56	16.07	16.46	15.88
8	0.0806	17.81	0.7128	319.3	117.7	137.0	16.07	15.59	15.88	15.29

TABLE III

VALUES OF THE CONSIDERED PIECEWISE SOLUTION DURING DESCENT. THE VALUES OF γ AND E ARE THE DESCENT ANGLE AND LIFT-TO-DRAG RATIO AT THE BEGINNING OF EACH PIECE, RESPECTIVELY, AND ρ AND a ARE THE MEAN VALUES OF THE AIR DENSITY AND SPEED OF SOUND OF EACH PIECE

Piece	γ (rad)	E (-)	ρ (kg/m^3)	a (m/s)	t_s (s)	t_e (s)	η_s (m/s)	η_e (m/s)	$\eta_{\text{Piano-X}}$ (m/s)	
1	−0.0569	16.08	0.4748	304.4	0.0	23.0	−13.40	−13.26	−13.40	−13.24
2	−0.0571	16.12	0.4926	305.7	23.0	46.0	−13.26	−13.12	−13.24	−13.10
3	−0.0574	16.13	0.5106	307.0	46.0	69.0	−13.12	−12.99	−13.10	−12.96
4	−0.0576	16.10	0.5290	308.3	69.0	93.0	−12.99	−12.86	−12.96	−12.83
5	−0.0579	16.06	0.5485	309.6	93.0	117.0	−12.86	−12.73	−12.83	−12.73
6	−0.0584	16.03	0.5684	311.0	117.0	141.0	−12.73	−12.61	−12.73	−12.62

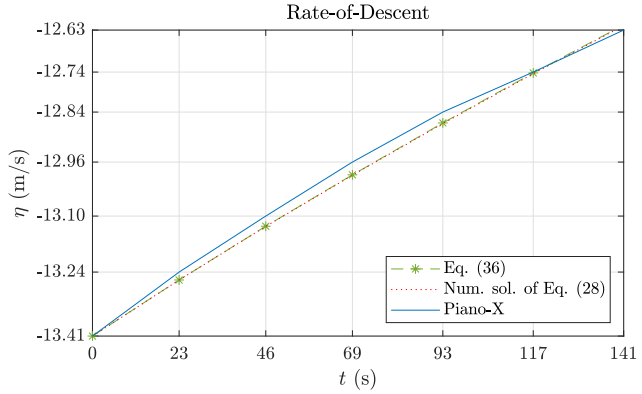

Fig. 2. The aircraft's rate-of-descent is represented for our mathematical model and Piano-X.

TABLE IV

VALUES OF THE AIRCRAFT'S FUEL CONSUMPTION GIVEN BY (38) FOR THE CLIMBING FLIGHT PHASE. THE TERM $\Delta m_f = m_f(\eta_e) - m_f(\eta_s)$ REPRESENTS THE AMOUNT OF FUEL CONSUMED FOR EACH PIECE, WHICH ADDED UP GIVES THE TOTAL AMOUNT OF FUEL CONSUMED

Piece	t_s (s)	t_e (s)	η_s (m/s)	η_e (m/s)	Δm_f (kg)
1	0.0	15.3	19.83	19.20	58.76
2	15.3	31.0	19.20	18.62	57.88
3	31.0	47.3	18.62	18.08	57.68
4	47.3	64.0	18.08	17.56	56.73
5	64.0	81.3	17.56	17.05	56.43
6	81.3	99.2	17.05	16.56	56.05
7	99.2	117.7	16.56	16.07	55.61
8	117.7	137.0	16.07	15.59	55.68

corresponds to a 0.0025%. Therefore, we conclude that the piecewise closed-form solution given by (36) provides a very good approximation of the actual solution of (23). Analogously, if we compare (36) with the values of the aircraft's rate-of-climb provided by Piano-X, we can notice that the maximum relative difference between both also occurs at $t_f = 137$ s and is equal to 1.8%.

Similarly, Figure 2 presents the piecewise closed-form solution given by (36), along with the numerical solution of (28) and the values of the aircraft's rate-of-descent provided by Piano-X. Again, the numerical solution of (28) was computed using the `ode45` numerical solver of MATLAB®. The maximum relative difference between (36) and (28) occurs at $t_f = 117$ s with a value of 0.01%. From this, we again conclude that the piecewise closed-form solution given by (36) provides a very good approximation of the actual solution of (28). Analogously, the comparison of (36) with the values of the aircraft's rate-of-descent provided by Piano-X shows that the maximum relative difference between both occurs at $t_f = 69$ s and is equal to 0.25%.

We can therefore conclude that our proposed mathematical model resembles with accuracy the results provided by Piano-X for the calculation of the aircraft's rate-of-climb and rate-of-descent.

We now provide in Table IV the piecewise closed-form solution of the aircraft's fuel consumption given by (38) for the climbing flight phase. Notice that Table IV puts together both the results obtained for the aircraft's rate-of-climb and fuel consumption. We will use this values in order to plot the time evolution of the fuel consumption.

Table V provides the piecewise closed-form solution of the aircraft's fuel consumption given by (38) for the descent flight phase, its values are also used to plot the time evolution of the fuel consumption.

Figure 3 shows the aircraft's fuel consumption given by (38) and by Piano-X for the climbing flight phase. The total amount of fuel consumed given by our mathematical model

Authorized licensed use limited to: TECNUN-UNIVERSIDAD DE NAVARRA. Downloaded on February 12,2024 at 08:33:46 UTC from IEEE Xplore. Restrictions apply.

This article has been accepted for inclusion in a future issue of this journal. Content is final as presented, with the exception of pagination.

TABLE V

VALUES OF THE AIRCRAFT'S FUEL CONSUMPTION GIVEN BY (38) FOR THE DESCENT FLIGHT PHASE. THE TERM $\Delta m_f = m_f(\eta_e) - m_f(\eta_s)$ REPRESENTS THE AMOUNT OF FUEL CONSUMED FOR EACH PIECE, WHICH ADDED UP GIVES THE TOTAL AMOUNT OF FUEL CONSUMED

Piece	t_s (s)	t_e (s)	η_s (m/s)	η_e (m/s)	Δm_f (kg)
1	0.0	23.0	−13.40	−13.26	5.08
2	23.0	46.0	−13.26	−13.12	5.00
3	46.0	69.0	−13.12	−12.99	4.90
4	69.0	93.0	−12.99	−12.86	4.97
5	93.0	117.0	−12.86	−12.73	4.84
6	117.0	141.0	−12.73	−12.61	4.75

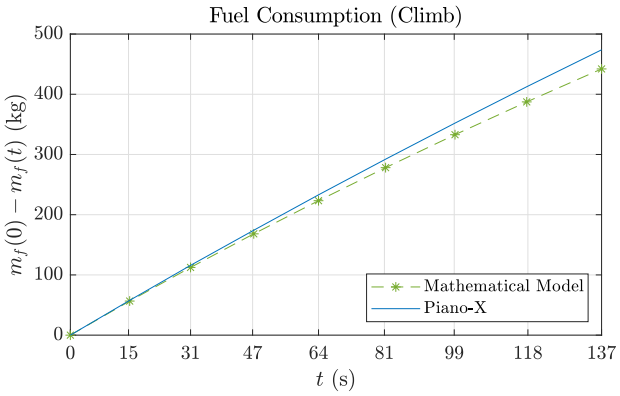

Fig. 3. The aircraft's fuel consumption during climb is represented for our mathematical model and Piano-X.

is of 442 kg and the corresponding value given by Piano-X is of 474 kg, which means a 6.7% of relative difference exists between both values.

Figure 4 presents the aircraft's fuel consumption given by (38) and by Piano-X for the descent flight phase. The total amount of fuel consumed given by our mathematical model and by Piano-X are of 29.56 kg and 29.40 kg, respectively, meaning that both values have a relative difference of 0.54%. Notice that the fuel consumption during the climbing flight phase is nearly fifteen times that of the descent flight phase, this is mainly due to the thrust configuration of each flight phase, which, in the case of the descent phase, corresponds to the idle configuration.

From this, we conclude that our mathematical model provides an accurate calculation of the aircraft's fuel consumption during the climbing and descent flight phases.

In the next section, an application of our mathematical model is presented for the calculation of pollutant gas emissions for the climbing flight phase.

V. APPLICATION: POLLUTANT GAS EMISSIONS CALCULATION

In this section, we obtain from our mathematical model a closed-form expression that enables the calculation of pollutant gas emissions of a jet engine aircraft during the climbing flight phase. The closed-form expression is given by

$$p_i = EI_i \left[m_f(t_s) - m_f(t_e) \right], \tag{39}$$

where p_i is the mass of pollutant gas emitted, EI_i is the emission index and i the corresponding chemical component.

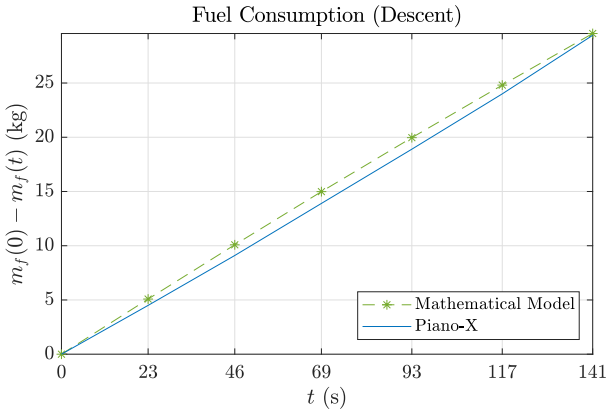

Fig. 4. The aircraft's fuel consumption during descent is represented for our mathematical model and Piano-X.

TABLE VI

THE DESIGNATION FOR THE SHORT-, MID- AND LONG-HAUL FLIGHTS IS PRESENTED, ALONG WITH ITS RESPECTIVE RANGE AND DEPARTURE AND ARRIVAL AIRPORT

Designation	Range (nmi)	Departure Airport	Arrival Airport
A	180	Penang (WMKP)	Kuala Lumpur (WMKK)
B	1,325	Louisville (KSDF)	Mexico City (MMMX)
C	2,820	Louisville (KSDF)	Anchorage (PANC)

Substituting (38) in (39) brings

$$p_i = EI_i \frac{\rho^{m+n}}{\mathsf{k}_3} \left(\epsilon_1(\eta_e - \eta_s) + \epsilon_2(\eta_e^2 - \eta_s^2) + \epsilon_3(\eta_e^3 - \eta_s^3) \right) + EI_i \frac{\rho^{m+n}}{\mathsf{k}_3} \left(\epsilon_4 \ln \left| \frac{\eta_e - r_1}{\eta_s - r_1} \right| - \epsilon_5 \ln \left| \frac{\eta_e - r_2}{\eta_s - r_2} \right| \right). \tag{40}$$

We recall that we have divided the climbing flight phase in altitude segments. Hence, (40) is a piecewise closed-form expression of the mass of pollutant gas emitted.

We now apply (40) for the calculation of carbon dioxide emissions (CO_2) for three example routes. These example routes were observed in the FlightRadar24 [37] platform and correspond to a freighter airline that has the Boeing 767-300ER as one of its cargo aircraft. Such routes are shown in Table VI.

Table VII shows the main input data and results for the climbing flight phase. The first column represents the designation for a short-, mid-, and long-haul flight as A, B and C, respectively, and t_f is the time elapsed from h_0 to h_f, with $h_0 = 457$ m. The term $(\Delta m_f)_{tot}$ is the total fuel consumption, which is the sum of fuel consumption per each piece. Likewise, the term $(p_{CO_2})_{tot}$ is the total mass of emitted CO_2, which is the sum of emitted CO_2 per each piece. The emission index of CO_2, that is, the grams of CO_2 emitted per kilogram of fuel consumed, has a value of $EI_{CO_2} = 3160$ [38].

In Table VIII we present, for the same routes, the fuel consumption and pollutant gas emissions for the take-off and cruising flight phases, whose values are obtained from the closed-form expressions presented in [20] and [21].

From Tables VII and VIII, we see that, for flight A, the total CO_2 emissions are of 5,948.9 kg, where the climbing flight phase represents a 45.3% which is comparable to the cruising flight phase which represents a 50.0%. For flight B, the total CO_2 emissions are of 36,026.8 kg, from which the

Authorized licensed use limited to: TECNUN-UNIVERSIDAD DE NAVARRA. Downloaded on February 12,2024 at 08:33:46 UTC from IEEE Xplore. Restrictions apply.

This article has been accepted for inclusion in a future issue of this journal. Content is final as presented, with the exception of pagination.

TABLE VII

A SUMMARY OF THE APPLICATION INPUT DATA AND RESULTS FOR THE CLIMBING FLIGHT PHASE. AIRCRAFT FUEL CONSUMPTION AND CO_2 EMISSIONS ARE PRESENTED IN THE $(\Delta m_f)_{tot}$ AND $(p_{CO_2})_{tot}$ COLUMNS, RESPECTIVELY

	Climb			
	t_f (s)	h_f (m)	$(\Delta m_f)_{tot}$ (kg)	$(p_{CO_2})_{tot}$ (kg)
A	258	6,408	852.1	2,692.7
B	526	8,766	1,520.7	4,805.4
C	580	8,400	1,733.8	5,478.8

TABLE VIII

A SUMMARY OF THE RESULTS FOR THE TAKE-OFF AND CRUISING FLIGHT PHASES. AIRCRAFT FUEL CONSUMPTION AND CO_2 EMISSIONS ARE PRESENTED IN THE m_f AND p_{CO_2} COLUMNS, RESPECTIVELY

	Take-off		Cruise	
	m_f (kg)	p_{CO_2} (kg)	m_f (kg)	p_{CO_2} (kg)
A	89.4	282.5	941.1	2,973.8
B	125.0	395.0	9,755.2	30,826.4
C	155.8	492.3	23,799.0	75,204.8

climbing flight phase represents a 13.3% and the cruising flight phase a 85.5%. Moreover, flight C has a total CO_2 emissions of 81,175.9 kg, where the climbing and cruising flight phases represent a 6.7% and 92.6%, respectively. Notice that, in the case of short-haul flights, the climbing phase CO_2 emissions account for a significant portion of total flight emissions. Whereas, for the mid- and long-haul flights, the climbing phase CO_2 emissions represent a lower portion of the total emitted CO_2 due to the fact that the cruising flight phase is longer in time duration.

Observe that (40) is a tool that provides a rapid means for calculating the aircraft pollutant emissions, in particular for the case of CO_2.

VI. CONCLUSION

The main objective of this paper was to develop a mathematical model for the fuel consumption of a jet engine aircraft during the climbing and descent flight phases. To this end, first order non-linear ordinary differential equations were obtained from the equations of motion of such flight phases, with the aircraft's rate-of-climb and rate-of-descent as a function of time, respectively. Such non-linear nature precludes the possibility of finding a closed-form solution, therefore, what we propose is the piecewise solution of both non-linear ordinary differential equations, where a closed-form solution is obtained for each piece.

In Section III, we presented the piecewise closed-form solution of the aircraft's fuel consumption that provides the closed-form relationship between the aircraft's fuel consumption and aerodynamic, engine and design parameters. In order to check its validity, an example route was simulated and the fuel consumption results provided by our mathematical model and by the Piano-X software were compared. The results of our mathematical model prove to be very accurate to the results of the Piano-X software.

Our mathematical model finds application in the calculation of pollutant gas emissions, in particular of CO_2. Specifically, we have also presented a piecewise closed-form expression that provides the dependency between the mass of pollutant gas emitted and the aircraft's aerodynamic, engine and design parameters.

TABLE IX

THE VALUES OF f_i (WITH $i = \{1, 2\}$) DEPEND ON BOTH THE BYPASS RATIO λ AND THE MACH NUMBER $M(h, \eta)$

		f_1	f_2
$3 \leq \lambda \leq 6$	$0 < M(h,\eta) < 0.4$	1	0
	$0.4 < M(h,\eta) < 0.9$	0.88	-0.016
$\lambda = 8$	$0 < M(h,\eta) < 0.4$	1	0
	$0.4 < M(h,\eta) < 0.9$	0.89	-0.014

With our mathematical model presented in this paper, along with the mathematical models presented in [20] and [21], one can obtain an accurate calculation of the jet engine aircraft fuel consumption during the climbing, descent, take-off and cruising flight phases, respectively.

APPENDIX A

In this appendix we show that $r_1 > 0$ and $r_2 < 0$. First we show that $F_1 > 0$.

From (12) we recall that

$$F_1 = N_e F_{N,0}(f_1 + f_2\lambda)\rho_0^{-n}, \tag{41}$$

with $N_e, F_{N,0}, \lambda, \rho_0, \gamma > 0$.

As stated in Section II-B, the specific parameters f_i (with $i = \{1, 2\}$) are obtained from [31, p. 67] and are presented in Table IX:

If $f_1 = 1$ and $f_2 = 0$, $f_1 + f_2\lambda > 0$. If $f_1 = 0.88$ and $f_2 = -0.016$, $f_1 + f_2\lambda > 0$ whenever $\lambda < 55$. If $f_1 = 0.89$ and $f_2 = -0.014$, $f_1 + f_2\lambda > 0$ whenever $\lambda < 63.57$.

Hence, we conclude that $F_1 > 0$ for $\lambda \in [3, 6] \cup \{8\}$.

As $F_1 > 0$ then $\mathsf{k}_1 > 0$. From (32) we have that $\mathsf{k}_3 < 0$ and therefore $\mathsf{k}_2^2 - 4\mathsf{k}_1\mathsf{k}_3 > 0$.

Suppose that $\mathsf{k}_2 \geq 0$. Then, $r_1 > 0$ and since $-\mathsf{k}_2 + \sqrt{\mathsf{k}_2^2 - 4\mathsf{k}_1\mathsf{k}_3} > -\mathsf{k}_2 + \sqrt{\mathsf{k}_2^2} = 0$, $r_2 < 0$.

Suppose that $\mathsf{k}_2 < 0$. Then, $r_2 < 0$ and since $-\mathsf{k}_2 - \sqrt{\mathsf{k}_2^2 - 4\mathsf{k}_1\mathsf{k}_3} > -\mathsf{k}_2 - \sqrt{\mathsf{k}_2^2} = 0$, $r_1 > 0$.

APPENDIX B

From the *Speed and Flight Levels* adjustment, the *Cruise Mach* is set to 0.8 and the *Available Flight Levels* is set to 350 (which is represented in flight level (FL) notation). The *Climb Speed* and *Climb Mach* are set to standard climb values. As for the *Basic Design Weights*, the operating empty mass is set to $m_{oe} = 93,032$ kg. Other adjustments such as the *Thrust. Drag. Fuel Flow*, *Emission Indices* and *Reserves and Allowances* remained in their default values.

The results are obtained from the *Detailed Flight Profile*, which is set to a specific *Range* and *Payload* of $2,145$ nmi and $m_{py} = 13,552$ kg, respectively. Notice that the sum of the operating empty and payload masses, multiplied by the gravity's acceleration, i.e. $(m_{oe} + m_{py})g$, represents the fixed-weight term W_0 in (3). As for the *Point Performance*,

Authorized licensed use limited to: TECNUN-UNIVERSIDAD DE NAVARRA. Downloaded on February 12,2024 at 08:33:46 UTC from IEEE Xplore. Restrictions apply.

This article has been accepted for inclusion in a future issue of this journal. Content is final as presented, with the exception of pagination.

the corresponding values of Mach, Altitude and Weight from the climbing flight segment are provided as input in order to obtain aircraft parameters such as the rate-of-climb, climbing angle (γ) or lift-to-drag ratio (E). The same is done for the descent flight segment in order to obtain aircraft parameters such as the rate-of-descent, descent angle (γ) or lift-to-drag ratio (E).

REFERENCES

[1] Statista. *Total Fuel Consumption of Commercial Airlines Worldwide Between 2005 and 2022*. Accessed: Jun. 6, 2022. [Online]. Available: https://www.statista.com/statistics/655057/fuel-consumption-of-airlines-worldwide/

[2] Statista. *Annual Growth in Global Air Traffic Passenger Demand From 2006 to 2022*. Accessed: Jun. 6, 2022. [Online]. Available: https://www.statista.com/statistics/193533/growth-of-global-air-traffic-passenger-demand/

[3] Air Transportation Action Group (ATAG). *Facts & Figures 2019*. Accessed: Jun. 15, 2022. [Online]. Available: https://data.worldbank.org/indicator/IS.AIR.PSGR?end=2019&start=1970&view=chart

[4] A. Filippone, *Advanced Aircraft Flight Performance*. Cambridge, U.K.: Cambridge Univ. Press, 2012.

[5] B. P. Collins, "Estimation of aircraft fuel consumption," *J. Aircr.*, vol. 19, no. 11, pp. 969–975, Nov. 1982, doi: 10.2514/3.44799.

[6] A. Trani, F. Wing-Ho, G. Schilling, H. Baik, and A. Seshadri, "A neural network model to estimate aircraft fuel consumption," in *Proc. AIAA 4th Aviation Technol., Integr. Operations (ATIO) Forum*, 2004, pp. 6401–6424. doi: 10.2514/6.2004-6401.

[7] S. Baumann and U. Klingauf, "Modeling of aircraft fuel consumption using machine learning algorithms," *CEAS Aeronaut. J.*, vol. 11, no. 1, pp. 277–287, Jan. 2020, doi: 10.1007/s13272-019-00422-0.

[8] G. Li, "Machine learning in fuel consumption prediction of aircraft," in *Proc. 9th IEEE Int. Conf. Cognit. Informat. (ICCI)*, Jul. 2010, pp. 358–363, doi: 10.1109/COGINF.2010.5599714.

[9] W. Zixuan, Z. Ning, H. Weijun, and Y. Sheng, "Study on prediction method of flight fuel consumption with machine learning," in *Proc. IEEE Int. Conf. Inf. Technol., Big Data Artif. Intell. (ICIBA)*, vol. 1, Nov. 2020, pp. 624–627, doi: 10.1109/ICIBA50161.2020.9277445.

[10] A. Antonakis, T. Nikolaidis, and P. Pilidis, "Multi-objective climb path optimization for aircraft/engine integration using particle swarm optimization," *Appl. Sci.*, vol. 7, no. 5, p. 469, Apr. 2017, doi: 10.3390/app7050469.

[11] H. Zhang and Liu. Zhang, "Fuel consumption model of the climbing phase of departure aircraft based on flight data analysis," *Sustainability*, vol. 11, no. 16, p. 4362, Aug. 2019, doi: 10.3390/su11164362.

[12] T. Baklacioglu, "Fuel flow-rate modelling of transport aircraft for the climb flight using genetic algorithms," *Aeronaut. J.*, vol. 119, no. 1212, pp. 173–183, Feb. 2015, doi: 10.1017/s0001924000010320.

[13] L. Jiaxue and M. Tao, "A method of aircraft fuel consumption performance evaluation based on RELAX signal separation," in *Proc. IEEE Int. Conf. Cyber Technol. Autom., Control, Intell. Syst. (CYBER)*, Jun. 2015, pp. 1433–1437, doi: 10.1109/CYBER.2015.7288154.

[14] R. Dalmau, X. Prats, A. Ramonjoan, and S. Soley, "Estimating fuel consumption from radar tracks: A validation exercise using FDR and radar tracks from descent trajectories," *CEAS Aeronaut. J.*, vol. 11, no. 2, pp. 355–365, Jun. 2020, doi: 10.1007/s13272-020-00441-2.

[15] H. Aygun and O. Turan, "Environmental impact of an aircraft engine with exergo-life cycle assessment on dynamic flight," *J. Cleaner Prod.*, vol. 279, Jan. 2021, Art. no. 123729, doi: 0.1016/j.jclepro.2020.123729.

[16] A. Kaba, H. Aygun, and O. Turan, "Multi-dimensional energetic performance modeling of an aircraft engine with the aid of enhanced least–squares estimation based genetic algorithm method," *J. Thermal Anal. Calorimetry*, vol. 147, no. 10, pp. 5913–5935, May 2022, doi: 10.1007/s10973-021-10922-z.

[17] I. Metz, J. Hoekstra, J. Ellerbroek, and D. Kügler, "Aircraft performance for open air traffic simulations," in *Proc. AIAA Model. Simul. Technol. Conf.*, Jun. 2016, p. 3522, doi: 10.2514/6.2016-3522.

[18] J. Sun, J. M. Hoekstra, and J. Ellerbroek, "OpenAP: An open-source aircraft performance model for air transportation studies and simulations," *Aerospace*, vol. 7, no. 8, p. 104, Jul. 2020, doi: 10.3390/aerospace7080104.

[19] K. Seymour, M. Held, G. Georges, and K. Boulouchos, "Fuel estimation in air transportation: Modeling global fuel consumption for commercial aviation," *Transp. Res. D, Transp. Environ.*, vol. 88, Nov. 2020, Art. no. 102528, doi: 10.1016/j.trd.2020.102528.

[20] F. Velásquez-SanMartín, X. Insausti, M. Zárraga-Rodríguez, and J. Gutiérrez-Gutiérrez, "A mathematical model for the analysis of jet engine fuel consumption during aircraft take-off," in *Proc. IEEE Aerosp. Conf. (AERO)*, Big Sky, MT, USA, Mar. 2022, pp. 1–10, doi: 10.1109/AERO53065.2022.9843276.

[21] F. Velásquez-SanMartín, X. Insausti, M. Zárraga-Rodríguez, and J. Gutiérrez-Gutiérrez, "A mathematical model for the analysis of jet engine fuel consumption during aircraft cruise," *Energies*, vol. 14, no. 12, p. 3649, Jun. 2021, doi: 10.3390/en14123649.

[22] LISSYS Limited. *Piano-X*. Accessed: May 10, 2022. [Online]. Available: https://www.lissys.uk/

[23] M. S. Ryerson, M. Hansen, L. Hao, and M. Seelhorst, "Landing on empty: Estimating the benefits from reducing fuel uplift in U.S. civil aviation," *Environ. Res. Lett.*, vol. 10, no. 9, Sep. 2015, Art. no. 094002, doi: 10.1088/1748-9326/10/9/094002.

[24] A. Skowron, D. S. Lee, and R. R. De León, "The assessment of the impact of aviation NO_x on ozone and other radiative forcing responses—The importance of representing cruise altitudes accurately," *Atmos. Environ.*, vol. 74, pp. 159–168, Aug. 2013, doi: 10.1016/j.atmosenv.2013.03.034.

[25] L. Dray, "Time constants in aviation infrastructure," *Transp. Policy*, vol. 34, pp. 29–35, Jul. 2014, doi: 10.1016/j.tranpol.2014.02.016.

[26] P. Krammer, L. Dray, and M. O. Köhler, "Climate-neutrality versus carbon-neutrality for aviation biofuel policy," *Transp. Res. D, Transp. Environ.*, vol. 23, pp. 64–72, Aug. 2013, doi: 10.1016/j.trd.2013.03.013.

[27] F. Svensson, A. Hasselrot, and J. Moldanova, "Reduced environmental impact by lowered cruise altitude for liquid hydrogen-fuelled aircraft," *Aerosp. Sci. Technol.*, vol. 8, no. 4, pp. 307–320, Jun. 2004, doi: 10.1016/j.ast.2004.02.004.

[28] J. M. Collins and D. McLarty, "All-electric commercial aviation with solid oxide fuel cell-gas turbine-battery hybrids," *Appl. Energy*, vol. 265, May 2020, Art. no. 114787, doi: 10.1016/j.apenergy.2020.114787.

[29] T. M. Young, *Performance of the Jet Transport Airplane: Analysis Methods, Flight Operations and Regulations*. Hoboken, NJ, USA: Wiley, 2018.

[30] P. M. Sforza, *Commercial Airplane Design Principles*, Waltham, MA, USA: Butterworth-Heinemann, 2014.

[31] D. Howe, *Aircraft Conceptual Design Synthesis*. Hoboken, NJ, USA: Wiley, 2000.

[32] M. H. Sadraey, *Aircraft Performance: An Engineering Approach*, Boca Raton, FL, USA: CRC Press, 2017.

[33] P. P. Walsh and P. Fletcher, *Gas Turbine Performance*. Malden, MA, USA: Blackwell Science, 2004.

[34] The Boeing Company. *Company, Boeing 767 Airplane Characteristics for Airport Planning (2005)*. p. 12. Accessed: May 26, 2022. [Online]. Available: http://www.boeing.com/assets/pdf/commercial/airports/acaps/767.pdf

[35] L. Jenkinson, P. Simpkin, and D. Rhodes, *Civil Jet Aircraft Design*, Waltham, MA, USA: Butterworth-Heinemann, 1999. Accessed: May 26, 2022. [Online]. Available: https://booksite.elsevier.com/9780340741528/appendices/default.htm

[36] General Electric. *Type-Certificate Data Sheet, CF6-80C2B2*. Accessed: May 26, 2022. [Online]. Available: https://www.easa.europa.eu/en/downloads/136365/en

[37] *FlightRadar24*. Accessed: Jun. 15, 2022. [Online]. Available: https://www.flightradar24.com

[38] U. Schumann, *Aircraft Emissions*, Chichester, U.K.: Wiley, 2002. Accessed: Jun. 22, 2022. [Online]. Available: https://elib.dlr.de/9477/1/arem.pdf

Authorized licensed use limited to: TECNUN-UNIVERSIDAD DE NAVARRA. Downloaded on February 12,2024 at 08:33:46 UTC from IEEE Xplore. Restrictions apply.

This article has been accepted for inclusion in a future issue of this journal. Content is final as presented, with the exception of pagination.

Francisco Velásquez-SanMartín was born in Tegucigalpa, Honduras. He received the industrial engineering degree in 2018 and the Sc.M. degree in industrial engineering from the University of Navarra, Donostia-San Sebastián, Spain, in 2020. He is currently pursuing the Ph.D. degree in applied engineering, specifically in developing a mathematical model that studies the fuel consumption of a jet engine aircraft during its different flight phases. His research interests include applied mathematics to physical systems.

Xabier Insausti was born in Beasain, Spain. He received the degree in telecommunications engineering from the University of Navarra, Donostia-San Sebastian, Spain, in 2009, the Sc.M. degree in advanced mathematics from UNED, Madrid, Spain, in 2013, and the Ph.D. degree in telecommunications engineering from the University of Navarra, in 2013. He is currently an Associate Professor with Tecnun, University of Navarra. His research interests include matrix analysis applied to problems in statistical signal processing, distributed computation, telecommunications, and information theory.

Marta Zárraga-Rodríguez was born in Oviedo, Spain. She received the B.Sc. and the M.Sc. degree in industrial engineering in 1993, a Ph.D. degree in industrial engineering in 1999 and a Ph.D. degree in applied engineering in 2017 from the University of Navarra, Donostia-San Sebastián, Spain. Currently, she is an Assistant Professor at Tecnun, University of Navarra, Donostia-San Sebastián, Spain. Her research interests include matrix analysis applied to problems in statistical signal processing, distributed computation, and information theory.

Jesús Gutiérrez-Gutiérrez (Senior Member, IEEE) was born in Granada, Spain. He received the degree in mathematics from the University of Granada, Granada, in 1999, and the Ph.D. degree in electronics and communications from the University of Navarra, Donostia-San Sebastian, Spain, in 2004. He is currently a Full Professor with Tecnun, University of Navarra. He is also the Head of the Department of Biomedical Engineering and Sciences, Tecnun. His research interests include matrix analysis applied to problems in statistical signal processing, distributed computation, and information theory.

Authorized licensed use limited to: TECNUN-UNIVERSIDAD DE NAVARRA. Downloaded on February 12,2024 at 08:33:46 UTC from IEEE Xplore. Restrictions apply.